INTERNATIONAL JOURNAL
FOR RESEARCH

IN APPLIED SCIENCE & ENGINEERING TECHNOLOGY

Investigation into Gas Pressure Variation at Inlet of a Converging-Diverging Nozzle

Ahmed H. Osman[1], Hesham E. Abdelhameed[2], Hamza H. Sobh[3]

[1]Assist. Prof., [2]Assoc. Prof, [3]Master Student, Mechanical Power Engineering Dept., Faculty of Engineering, Zagazig University, Zagazig 44519, EGYPT

Abstract: The future problem of oil loss is a major obstacle to the airline's companies. This research solves out this problem: solar or nuclear power plants use liquefied air; the liquefied air is used instead of hydrocarbon fuel by heating and then passing through the De Laval nozzle. This is the main reason for this investigation. This paper focuses on the nozzle design and the effect of inlet pressure change (for air) on the Mach number of the nozzle outlet. Two models were designed; the total pressure (gauge) of air at the entrance is equal to 9 & 11 bar. The change in the Mach number at the exit of the De Laval nozzle is observed in both models due to the change in the total pressure. The models were practically designed and applied. The results obtained from the practical models were compared with the theories of gas dynamics and ANSYS Fluent program. Total and static air pressure is measured at outlet of the nozzle. Experimentally, good results for air discharge in the nozzle were obtained and good agreement between numerical and experimental results.

Keywords: Mach number; Convergent-Divergent Nozzle; Pressure Variations.

NOMENCLATURE

A	cross section area, m^2	P_t	Absolute total pressure, bar
A_o	Outlet cross section area, m^2	P_{Sensor}	Sensor pressure
A^*	Throat cross section area, m^2	$P_{s,x}$	Static pressure at point X
a	Sound speed, m/s	$P_{s,y}$	Static pressure at point Y
a_o	Outlet Sound speed, m/s	$P_{t,x}$	Total pressure at point X
D_{inlet}	Nozzle inlet diameter, mm	$P_{t,y}$	Total pressure at point Y
D_{outlet}	Nozzle outlet diameter, mm	P_o	outlet static pressure (gauge), bar
D_{throat}	Nozzle throat diameter, mm	R	Gas constant
F	Thrust force (N) Newtons	T	Static temperature, K
M	Mach number	T_t	Total temperature, K
M_O	Nozzle outlet Mach number	T_o	Outlet Static temperature, K
M_x	Mach number at point X	V_o	Outlet velocity, m/s
M_y	Mach number at point Y	V	velocity, m/s
$\dot{m}$	Mass flow rate, Kg/s	V_{Sensor}	Sensor output voltage, volt
P	Absolute static pressure, bar	ρ	Density, kg/m^3
P_a	Atmospheric pressure	ρ_o	outlet density, kg/m^3
ρ_t	stagnation density, kg/m3	θ_{in}	Half angle of the converging nozzle, deg.
γ	Ratio of specific heat capacities	θ_{out}	Half angle of the diverging nozzle, deg.

I. INTRODUCTION

A number of studies presented experimental have been carried out with the goal of improving and use different applications for the nozzle system, such as T. Stoltenhoff et al. [1] they studied An Analysis of the Cold Spray Process and Its Coatings, the modeling of the gas and particle flow field for different nozzle geometries and process parameters in correlation with the results of the experiments reveals that adhesion only occurs when the powder particles exceed a critical impact velocity that is specific to the spray material.

Tien-Chien Jen, et al. [2] studied numerical investigations on cold gas dynamic spray Process with Nano- and micro size particles, the acceleration process of microscale and sub-microscale copper (Cu) and platinum (Pt) particles inside and outside De-Laval-Type nozzle is investigated. A numerical simulation. Manolo Pires [3] studied turbulence modeling and applications to aerospike plug

nozzle, a research on recent turbulence models considering the physical Reynolds stresses is proposed. Efficient state of the art numerical tools has been developed and are used for the simulation of increasingly complex flow fields. Flow fields varying plug nozzles are simulated for two-dimensional, axisymmetric configurations. Anisotropic models suffer from the same shortcomings than standard models because of the basic assumptions made in the Navier- Stokes equations. Gawehn et al. [4] studied Experimental and numerical analysis of the structure of pseudo-shock systems in laval nozzles with parallel side walls, the wall pressure distributions and high-speed schlieren videos recorded in the experiments are compared to the results of a steady and an unsteady numerical simulation. For the steady case, good agreement is found between the calculated and measured shock structure and pressure distribution along the primary nozzle wall, except for a remaining slight deviation in the shock position. For the unsteady case, in which asymmetric shock configurations are observed, deviations of the results with respect to the stochastic wall attachment of the shock system are given which indicate the necessity of further investigations on that topic. k.m. pandey, et al. [5] studied CFD analysis of conical nozzle for Mach 3 at various angles of divergence using Fluent software, the present study is aimed at investigating the supersonic flow in conical nozzle for Mach 3 at various degree of angle. The throat diameter and exit diameter is same for all nozzles. The flow is simulated using Fluent software. R. Lupoi and W. O' Neill 2010 [6] studied Deposition of Metallic Coatings on Polymer Surfaces using Cold Spray, In this method, a material in powder form is accelerated on passage through a converging-diverging nozzle to high speeds via a high pressure coaxial carrier gas jet. The high impact kinetic energy deforms the particles, which creates effective bonding to the substrate. Jamal Uddin et al. [7] prepared a computational study of supersonic flow through a converging diverging nozzle, computational solution has been obtained for Supersonic Flow through a Converging Diverging Nozzle. Various characteristics of compressible fluid flow through nozzle is analyzed and determined. The nozzle geometry is assumed as circular and axisymmetric and flow as two-dimensional flow. Pardhasaradhi Natta et al. [8] studied the Flow Analysis of Rocket Nozzle Using Computational Fluid Dynamics (CFD), study is aimed at investigating the supersonic flow in conical nozzle for Mach number 3 at various divergence degree of angle. The throat diameter and inlet diameter are same for all nozzles with various divergence degree of angles. SATYANARAYANA, et al. [9] studied the CFD analysis of Converging diverging nozzle, CFD analysis of flow within Convergent-Divergent supersonic nozzle of different cross sections rectangular, square and circular has been performed, analysis have been carried out in ANSYS FLUENT 12.0 and various contours like velocity, pressure, temperature have been taken and their variation according to different nozzles has been studied. Compared to square and circular nozzles, rectangular nozzle gives an increased velocity of about 23.93% and 24.47% respectively and an increased pressure drop of 22.93% and 23.97% respectively and an increased temperature drop of 42.56% and 43.68% respectively. It is found that fluid properties like velocity, pressure and temperature are largely dependent on the cross section of the nozzle which affects the flow within the nozzle and the extent of flow expansion.

H Pujowidodo, et al. [10] studied the Study of Converging-Diverging Nozzle for Improving the Impulse Momentum of Cross Flow Turbine in a Bio-Micro Power Plant, The analyze of momentum flux for rotating power turbine using integration thermodynamics and CFD models has shown that the smallest pressure ratio will increase the supersonic flow pass through the CD-nozzle with throat diameter 2 mm and outlet diameter 2.4 mm. For pressure ratio 0.5and temperature 200 °C of steam fluid, the maximum velocity that occurred was1.3Ma and mass flow was 0.978 kg/s (3.52 ton/hour). Flux could be increased by making larger cross-sectional area.

II. THEORETICAL WORK

In our work, we study the effect of changing the total pressure value at the entrance on the value of the static pressure, Mach number and thrust force at the exit, practically. Ratios of pressure, density and temperature can be related to the stagnation temperature, pressure and density at a given Mach number as seen in equations 1 – 3. and ratio across section area to cross section area at throat a given Mach number as seen in equation 4, and relation between the speed of the sound and the temperature as seen in equation 5, and the relation between gas velocity and sound speed as seen in equation 6.

$$\frac{T}{T_t} = \frac{1}{1 + \frac{\gamma - 1}{2} M^2} \tag{1}$$

$$\frac{P}{P_t} = \left[\frac{1}{1 + \frac{\gamma - 1}{2} M^2} \right]^{\frac{\gamma}{\gamma - 1}} \tag{2}$$

$$\frac{\rho}{\rho_t} = \left[\frac{1}{1 + \frac{\gamma - 1}{2} M^2} \right]^{\frac{1}{\gamma - 1}} \tag{3}$$

$$\frac{A}{A^*} = \frac{1}{M} \left[\frac{1 + \frac{\gamma - 1}{2}}{1 + \frac{\gamma - 1}{2} M^2} \right]^{\frac{-(\gamma+1)}{2(\gamma-1)}} \tag{4}$$

$$\mathbf{a = \sqrt{\gamma RT}} \tag{5}$$

$$\mathbf{V = M \, a} \tag{6}$$

The first model is theoretically designed to work at absolute total pressure 10.013 bar at inlet, absolute pressure at the outlet 1.45 bar and Mach number M=1.92 at the outlet. With a gradual decrease in absolute total pressure to less than 19.15% of $P_{t, x}$ ($P_{t, x}$ = 10.013 bar), Mach number is decreasing to the subsonic stage.

The second model is theoretically designed to work at absolute total pressure 12.013 bar at inlet, absolute static pressure 0.52 bar at the outlet and Mach number M=2.7 at the outlet. With a gradual decrease in absolute total pressure to less than 15.96 % of $P_{t, x}$ ($P_{t, x}$ = 10.013 bar), Mach number is decreasing to the subsonic stage.

III.   COMPUTATIONAL WORK

In the first model (more details about this model can be found in [11]), if the value of the input total pressure decreases, there is a decrease in output pressure, but when the absolute total pressure of the entrance decrease to the 1.91754 bar it is forming normal shock wave occurs within the nozzle after the throat, the gauge static pressure is increased from -0.0572 bar after the throat before normal shock wave to 0.0673 bar at the outlet as shown in the figure (1),the Mach number is decreased from 1.62 after the throat before normal shock wave to 1.07 at the outlet as shown in the figure (2), Flow is turning from supersonic flow to sonic flow. With a gradual decrease in absolute total pressure at inlet to less than 19.15 % of P_t 10.013 bar, Mach number is decreasing to the subsonic stage.
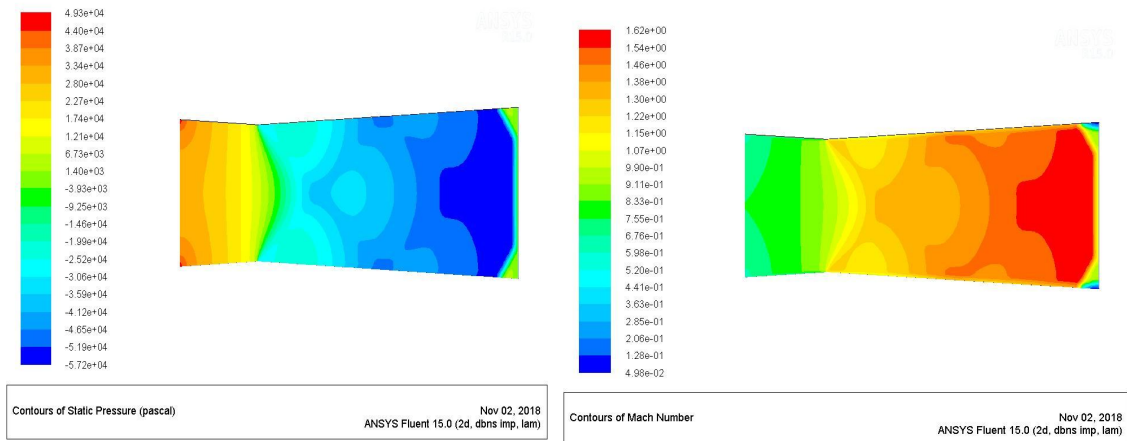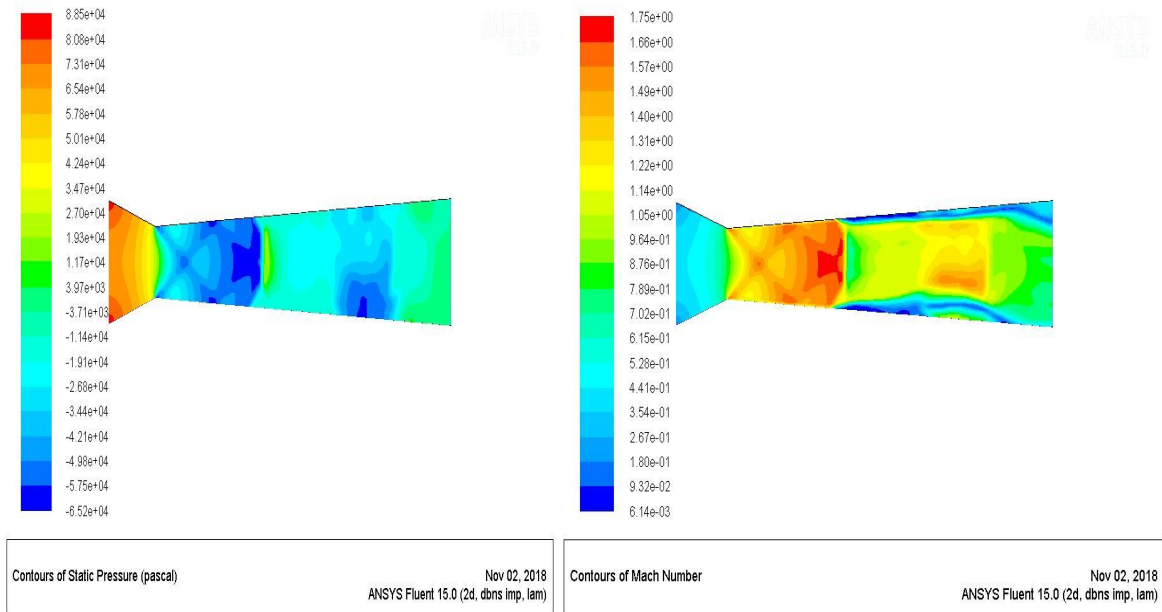

Figure 1 contour of gauge Static pressure (absolute total pressure 1.91754 bar at inlet)   Figure 2 contour of Mach number (absolute total pressure 1.91754 bar at inlet)

In second model when the value of the input total pressure decreases, there is a decrease in output pressure, but when the absolute total pressure of the entrance decreases to the 1.91754 bar it is forming normal shock wave occurs within the nozzle after the throat. The gauge static pressure is increasing from -0.0625 bar after the throat before normal shock wave to 0.193 bar at the outlet as shown in figure (3), The Mach number is decreased from 1.75 after the throat before normal shock wave to 1.02 at the outlet as shown in figure (4). Flow is turning from supersonic flow to sonic flow, with a gradual decrease in absolute total pressure at inlet to less than 15.96 % of P_t 12.013 bar, Mach number is decreasing to the subsonic stage.

International Journal for Research in Applied Science & Engineering Technology (IJRASET)
ISSN: 2321-9653; IC Value: 45.98; SJ Impact Factor: 7.177
Volume 7 Issue V, May 2019- Available at www.ijraset.com

Figure 3 contour of gauge Static pressure (absolute total pressure 1.91754 bar at inlet)   Figure 4 contour of Mach number (absolute total pressure 1.91754 bar at inlet)

IV. EXPERIMENTAL WORK

Figure (5) shows the layout of the test rig. Experiment parts. The system consists of the following components:

Figure 5 Test Rig

A. Air Supply (Compressor + tank)

B. Pitot Tube

The pitot tube was designed to measure the total pressure and the static pressure of the air after leaving the nozzle. A shock wave occurs to air during movement with speed more than sound sped inside the measuring tube. Total pressure $P_{t,y}$ is measured at point y and static pressure $P_{s,x}$ is measured at point x, Then calculate the Mach number value and total pressure $P_{t,x}$ Of Equations 7 and 8.
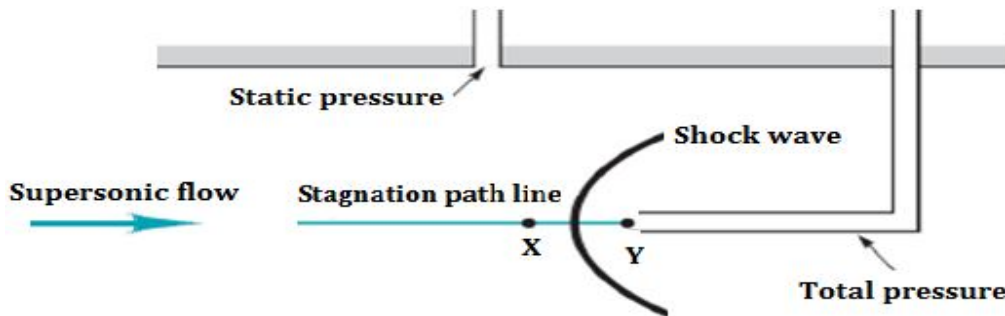

Figure 6 Pitot tube

$$\frac{P_{t,y}}{P_{s,x}} = \frac{[\frac{\gamma + 1}{2} M_x^2]^{\frac{\gamma}{\gamma-1}}}{[\frac{2\gamma}{\gamma + 1} M_x^2 - \frac{\gamma - 1}{\gamma + 1}]^{\frac{1}{\gamma-1}}} \qquad (7)$$

$$\frac{P_{s,x}}{P_{t,x}} = \left[\frac{1}{1 + \frac{\gamma - 1}{2}M_x^2}\right]^{\frac{\gamma}{\gamma-1}} \qquad (8)$$

C. Sensors

Two sensors to measure the total pressure and the static pressure, the pressure value corresponding to the voltage difference in the experiment range

$$P_{Sensor} = 6.25V_{Sensor} - 3.125 \qquad (9)$$

Measuring error ±1.5% FSO

$\frac{dp}{P_{fs}} = \pm 1.5\%$

$\frac{dp}{25} = \pm 1.5\%$

dp = ±0.375

In this experiment, maximum pressure equal 14.3 bar

Error $\frac{dp}{P} = \frac{\pm 0.375}{14.3} * 100 = \pm 2.62\%$

The pitot tube was designed to measure the total pressure and the static pressure of the air at the outlet of the nozzle. The pressure sensors were installed on the pitot tube to convert the pressure values to electrical signals and convert this value of the electrical signals.

D. Nozzle (Two Models)

Figure (7) shows a schematic drawing of the nozzle. Angles and dimensions of nozzles are shown in table (1).
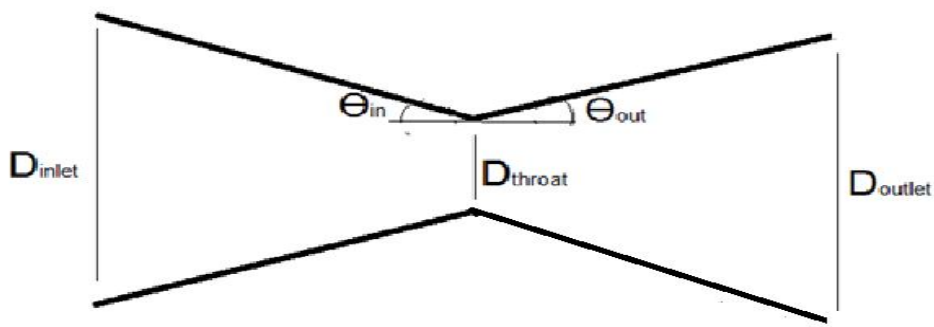

Figure 7 Nozzle

Table 1 Angles and dimensions of nozzles

	Model 1	Model 2
D_{inlet}	6 mm	9.7 mm
D_{throat}	5.57 mm	5.61 mm
D_{outlet}	7 mm	10 mm
θ_{in}	3.5 deg.	20 deg.
θ_{out}	3.5 deg.	3.5 deg.

E. Data Acquisition System

A data acquisition card from Data Translation model DT3001 with the following specifications 12-Bit, 330 KS/s, High-Speed DAQ Board with 16 Single Ended Analog Inputs. A modified version of another application [12] is used to acquire data. The modified application is programmed using TestPoint programming language.

V.   RESULTS & DISCUSSION

A. Mach Number

The first model is theoretically designed to work at absolute total pressure equal 10.013 bar at inlet, absolute pressure at the outlet equal 1.45 bar and Mach number M=1.92 at the outlet. It is found that the Mach number Mx equal 2.20711 when absolute total pressure $P_{t,x}$ equal 9.171099 bar and absolute static pressure at the outlet equal 0.848405 bar, the reason for increase in the value of the Mach number on the theoretical value due to lower value of the outlet pressure to less than the theoretical value. When gradual increase in absolute total pressure at inlet a gradual increase in the Mach number, when gradual decrease in absolute total pressure at inlet a gradual decrease in the Mach number occurs but remains in the supersonic stage. With a gradual decrease in absolute total pressure to less than 18.5% of $P_{t,x}$ ($P_{t,x}$ =10.013 bar), Mach number is decreasing to the subsonic stage.

In second model is theoretically designed to work at absolute total pressure equal 12.013 bar at inlet, absolute static pressure equal 0.52 bar at the outlet and Mach number M=2.7 at the outlet. It is found that the Mach number M_x equals 2.2845 when absolute total pressure $P_{t,x}$ equals 11.46942 bar and absolute static pressure 0.939758 bar at the outlet. Mach number M_x equals 2.4245 when absolute total pressure $P_{t,x}$ equals 13.81126 bar and absolute static pressure equals 0.90924 bar at the outlet. this due to the value of the outlet pressure is more than the theoretical value. When a gradual decrease in absolute total pressure at the inlet occurs; a gradual decrease in the Mach number occurs but remains in the supersonic stage.   With a gradual decrease in absolute total pressure to less than 16 % of $P_{t,x}$ ($P_{t,x =}$12.013 bar), Mach number is decreasing to the subsonic stage.

The previous models show the effect of the ratio between output static pressure (absolute) and total pressure (absolute) on the Mach number, in first model $\frac{P}{P_t}$ = 0.09251 at Mach number equal 2.207, in second model $\frac{P}{P_t}$ = 0.08194 at Mach number equal 2.4245, relationship between them is inverse.
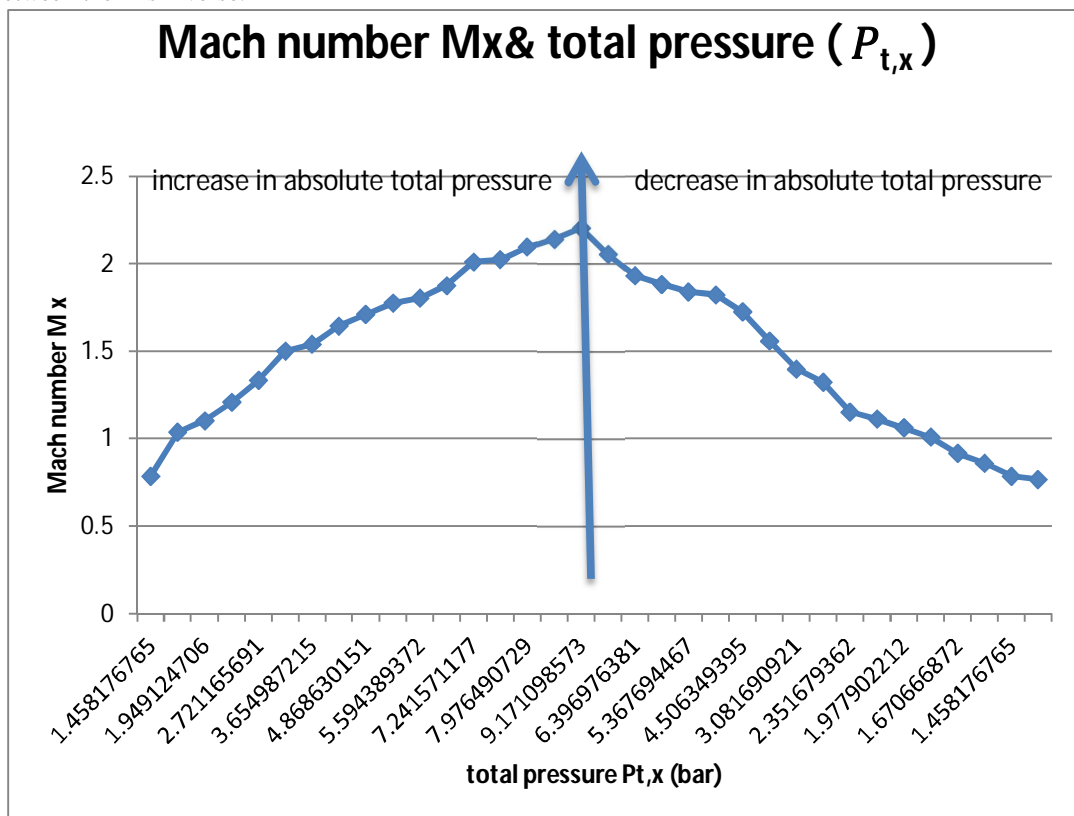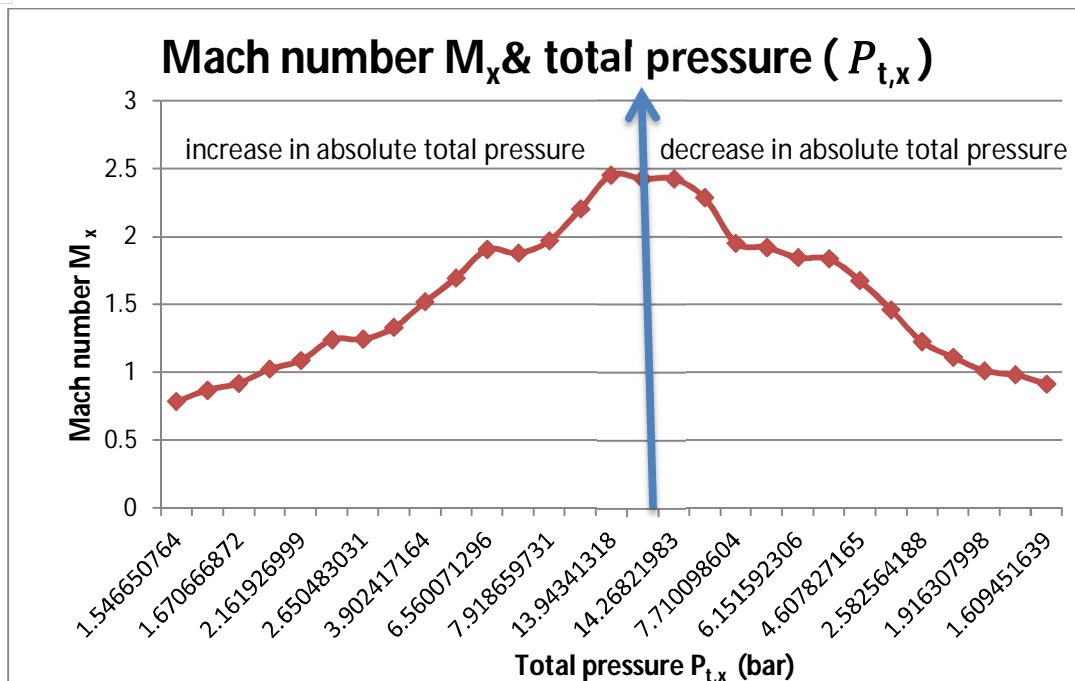

Figure 8 Mach number and total pressure model 1

Figure 9 Mach number with total pressure model 2

B. *Thrust Force (Newton's)*

In first model, thrust force equals 21.62772 N at absolute total pressure $P_{t,x}$ =9.171099 bar, absolute static pressure $P_{s,x}$=0.848205 bar and Mach number M_x = 2.20711, The thrust force gradually decreases with decrease in Mach number, because the thrust force is directly proportional to Mach number square as seen in equations 10 and 11.

$$F = \dot{m}\, v_o + (P_{Abs,out} - P_a)A_o \qquad (10)$$

$$\dot{m} = \rho_o A_o v_o \qquad (11)$$

$F = \rho_o A_o v_o * v_o + P_o A_o$

$F = \rho_o A_o v_o^2 + P_o A_o$

$F = \frac{P_{Abs,out}}{RT_o} A_o v_o^2 + P_o A_o$

$F = \frac{P_{Abs,out}}{RT_o} A_o M_O^2\, a_o^2 + P_o A_o$

$F = \frac{P_{Abs,out}}{RT_o} A_o M_O^2 \gamma RT_o + P_o A_o$

$F = \gamma A_o (P_O + P_a)M_O^2 + P_o A_o$

When outlet pressure is constant, or a small change occurs

$$F \propto M_o^2$$

Second model thrust force equals 53.35538 N at total pressure $P_{t,x}$ =11.46941705 bar , static pressure $P_{s,x}$=0.9397582 bar and Mach number M_x = 2.20711 .

Thrust force equal 57.95533 N at total pressure $P_{t,x}$ =13.81126 bar, static pressure $P_{s,x}$=0.90924 bar and Mach number M_x = 2.4245, The thrust force gradually decreases with decrease in Mach number. When the total pressure is less than work pressure of the nozzle, the outlet static pressure increases, Mach number and thrust force decrease as indicated in points A, B. When the total pressure increases, the outlet static pressure decreases, Mach number and thrust force increase as indicated in point C. This is compatible with the gas dynamics.

Table 2 Thrust force model 2

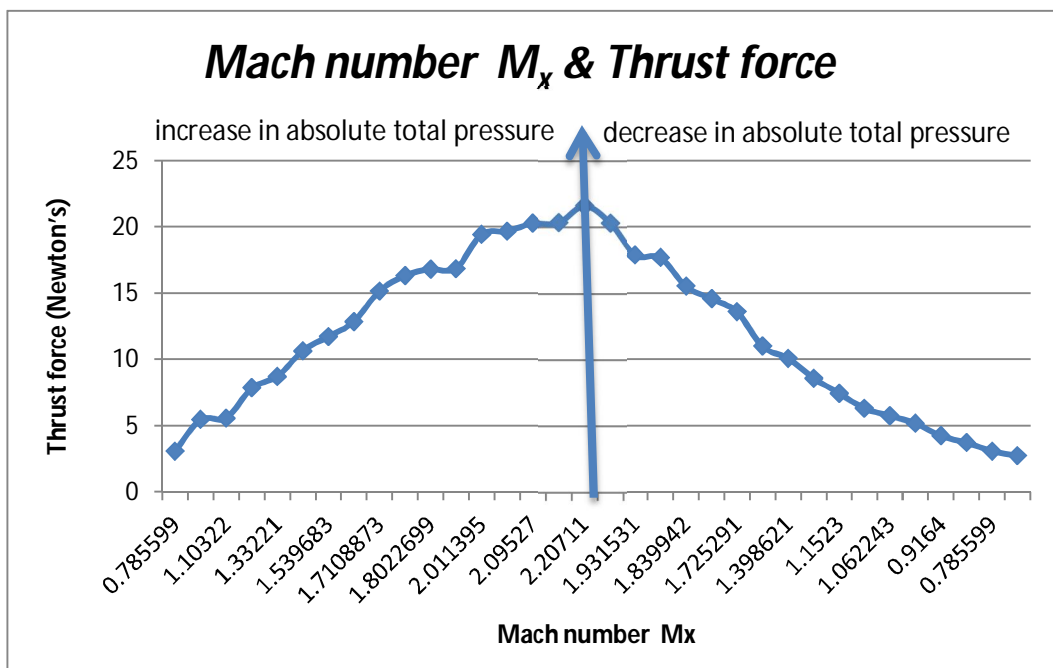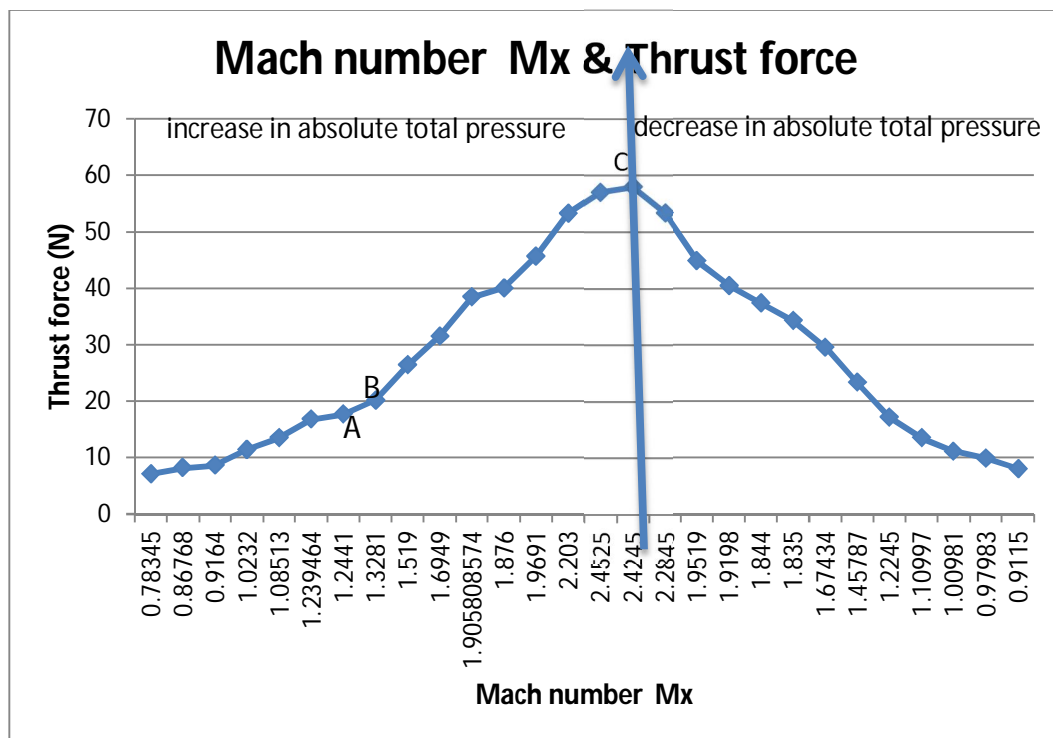| point	$P_o = P_{s,x}$	M	F	$P_{t,x}$
A	1.031311	1.2441	17.69615	2.650483
B	1.031311	1.3281	20.1464	2.96942
c	0.90924	2.4245	57.95533	13.81126

Figure 10 force and Mach number model 1

Figure 11 force and Mach number model 2

VI. CONCLUSION

To obtain a Mach number equal to one in the throat area, the total absolute pressure should be at least equal 1.91754 bar. When the output pressure is equal to the atmospheric pressure according to equation 12.

$$\frac{P}{P_t} = \left[\frac{2}{\gamma + 1}\right]^{\frac{\gamma}{\gamma - 1}} \tag{12}$$

Air usage instead of fuel in propulsion engines makes the results proximate to the gas dynamics, as it showed good results in the practical experience proximate to the theoretical results. The efficiency of the nozzle work is affected by the change of the total pressure at the inlet of the nozzle where the Mach number and thrust force increase with the slight increase in the inlet total pressure.

A. Future Work

Study the separation. And boundary layer of the fluid inside the converging diverging nozzle, which appeared in figure 4.

B. Acknowledgements

The authors would like to thank Prof. Mofreh Milad for his contribution of this work.

REFERENCES

[1] Stoltenhoff, T., H. Kreye, and H. Richter, An analysis of the cold spray process and its coatings. Journal of Thermal Spray Technology, 2002. 11(4): p. 542-550.

[2] Jen, T.-C., et al., Numerical investigations on cold gas dynamic spray process with nano-and microsize particles. International Journal of Heat and Mass Transfer, 2005. 48(21-22): p. 4384-4396

[3] Teeling, E.C., et al., A molecular phylogeny for bats illuminates biogeography and the fossil record. Science, 2005. 307(5709): p. 580-584.

[4] Gawehn, T., et al., Experimental and numerical analysis of the structure of pseudo-shock systems in laval nozzles with parallel side walls. Shock Waves, 2010. 20(4): p. 297-306.

[5] Pandey, K. and A. Singh, CFD analysis of conical nozzle for mach 3 at various angles of divergence with fluent software. International Journal of Chemical Engineering and Applications, 2010. 1(2): p. 179.

[6] Lupoi, R. and W. O'Neill, Deposition of metallic coatings on polymer surfaces using cold spray. Surface and Coatings Technology, 2010. 205(7): p. 2167-2173.

[7] Chowdhury, M., et al., Computational study of supersonic flow through a converging diverging nozzle. Engineering e-Transaction (ISSN 1823-6379), 2011. 6(1): p. 37-42.

[8] Natta, P., V.R. Kumar, and Y.H. Rao, Flow analysis of rocket nozzle using computational fluid dynamics (Cfd). Dynamics (Cfd), 2012. 2(5.(

[9] Satyanarayana, G., C. Varun, and S. Naidu, "CFD analysis of convergent-divergent nozzle". Acta Technica Corviniensis-Bulletin of Engineering, 2013. 6(3): p. 139.

[10] Pujowidodo, H., et al. "The Study of Converging-Diverging Nozzle for Improving the Impulse Momentum of Cross Flow Turbine in a Bio-Micro Power Plant". in IOP Conference Series: Earth and Environmental Science. 2018. IOP Publishing.

[11] Ahmed H. Osman, Hesham E. Abdelhameed, Hamza H.Sobh, "CFD Analysis of De Laval Nozzle Geometry & Effect of Gas Pressure Variation at the Entrance", International Journal for Research in Applied Science & Engineering Technology (IJRASET) Volume 6 Issue XII, p. 350-361,Dec 2018.

[12] Ahmed H. Osman and Magdy. M. Massoud, "Setting up a Data Acquisition System for Spark Engined", 1st Annual International Interdisciplinary Conference, AIIC 24-26 April, 2013, Azores, Portugal